Garcia-Garcia, D.; Garcia-Garcia, D.; Balart, R.; Strömberg, E.; Moriana, R. (2018). Reinforcing capability of cellulose nanocrystals obtained from pine cones in a biodegradable poly(3-hydroxybutyrate)/poly(e-caprolactone) (PHB/PCL) thermoplastic blend. European Polymer Journal. 104:10-18. https://doi.org/10.1016/j.eurpolymj.2018.04.036

"Reinforcing capability of cellulose nanocrystals obtained from pine cones in a biodegradable poly(3-hydroxybutyrate)/poly(ε-caprolactone) (PHB/PCL) thermoplastic blend"

Daniel Garcia-Garcia[1]*, Juan Lopez-Martinez[1], Rafael Balart[1], Emma Strömberg[3], Rosana Moriana[2,3]*

[1] *Instituto de Tecnología de Materiales-ITM*

Universitat Politècnica de València

Plaza Ferrandiz y Carbonell 1, 03801, Alcoy, Alicante (Spain)

[2] *School of Engineering Science*

HIS-University of Skövde, Skövde

Högskolevägen, 541 28, Skövde (Sweden)

[3] *School of Chemical Science and Engineering, Department of Fibre and Polymer Technology*

KTH-Royal Institute of Technology

SE-100 44, Stockholm (Sweden)

* Corresponding author: Rosana Moriana; Daniel Garcia-Garcia

E-mail: rosana@kth.se; dagarga4@epsa.upv.es

Tel.: (+46) 707595434; (+34) 96 652 84 34

Fax: (+34) 96 652 84 33

Abstract

In this work, different loads (3, 5 and 7 wt%) of pine cone cellulose nanocrystals (CNCs) were added to films of poly(3-hydroxybutyrate)/poly(ε-caprolactone) (PHB/PCL) blends with a composition of 75 wt% PHB and 25 wt% PCL (PHB_{75}/PCL_{25}). The films were obtained after solvent casting followed by melt compounding in an extruder and finally subjected to a thermocompression process. The influence of different CNCs loadings on the mechanical, thermal, optical, wettability and disintegration in controlled compost properties of the PHB_{75}/PCL_{25} blend was discussed. Field emission scanning electron microscopy (FESEM) revealed the best dispersion of CNCs on the polymeric matrix was at a load of 3 wt%. Over this loading, CNCs aggregates were formed enhancing the films fragilization due to stress concentration phenomena. However, the addition of CNCs improved the optical properties of the PHB_{75}/PCL_{25} films by increasing their transparency and accelerated the film disintegration in controlled soil conditions. In general, the blend with 3 wt% CNCs offers the best balanced properties in terms of mechanical, thermal, optical and wettability.

Keywords: poly(3-hydroxybutyrate); poly(ε-caprolactone); biodegradability; cellulose nanocrystals (CNCs); thermoplastic blends.

1. INTRODUCTION

The recent increase in the social concern about environmental issues together with the increasing price of fossil fuels due to petroleum depletion [1], has given a rise in the development of new environmentally friendly materials as it is the case of biodegradable polymers. Biodegradable polymers challenges are related to their relatively poor mechanical and thermal properties compared to petroleum-based commodities and engineering plastics, restricting their wide use in industrial application [2]. The reinforcement of biodegradable polymers with nanoparticles has recently been proposed as a strategy to overcome some of the above-mentioned drawbacks. Specifically, bio-based nanoscale particles have been used to reinforce thermoplastic biodegradable polymers, such as poly(lactic acid) (PLA), [3-5], poly(hydroxybutyrate) (PHB) [6], poly(ε-caprolactone) (PCL) [7, 8] and poly(butylene adipate-*co*-terephthalate) (PBAT) [9]. The improved thermo-mechanical performance of these nanoscale-reinforced polymer composites, together with their potential biodegradation, could lead these new materials to compete with many traditional petroleum-based polymers, such as polypropylene (PP), polyethylene or polyethylene terephthalate (PET) [10, 11].

Cellulose nanocrystals (CNCs) from residual biomass (food, agriculture and forest) may be defined as one of the most promising reinforcing agents in terms of biodegradability, renewability, abundance in nature, variety and price [12, 13]. These highly crystalline cellulose particles are obtained from lignocellulosic fibres generally through two main steps: first, an alkaline and bleaching treatment to isolate the cellulose fibres from the raw material and second, a hydrolytic treatment with acid which allows the selective removal of the amorphous cellulosic phase remaining the crystalline phase almost unaltered [14-16]. The physico-chemical properties of CNCs can vary widely, depending on the source of the cellulosic raw material and the conditions selected to perform the hydrolysis [17, 18]. In previous studies, pine cones fibres were selected as raw materials to produce CNCs and the influence of the hydrolytic time on their properties and the processing yield was evaluated [Daniel Garcia-Garcia, Rafael Balart, Juan Lopez-Martinez, Rosana Moriana, 2018, under review in cellulose journal]. Furthermore, the potential of using the pine cone CNCs as reinforcement in composites was discussed in terms of

aspect ratio, crystallinity and thermal stability. It is known that the influence of the matrix-reinforcement interface and compatibility is of foremost importance for the resulting performance of the composite materials. Therefore, in this study, we propose to evaluate the reinforcing capability of the pine cone CNCs in a biodegradable thermoplastic blend composed of 75% poly(3-hydroxybutyrate) and 25% poly(ε-caprolactone) (PHB_{75}/PCL_{25}). The overall effect of CNCs as reinforcement in thermoplastic composites highly depends on the percentage of loading nanoparticles and the particle dispersion in the polymer matrix [19]. The main challenge to overcome to design CNCs based composites is related to the poor dispersion of these nanoparticles in hydrophobic polymers due to their high hydrophilic nature [20, 21]. Chemical modification of the CNCs or the use of surfactants during the compounding step are the most used approaches to enhance the dispersion of CNCs on the polymeric matrix, avoiding the formation of aggregates [22, 23]. However, Wang *et al.* [24] shown how the chemical modification of CNCs could disrupt their crystalline structure with the subsequent decrease in rigidity. Another important challenge in using CNCs in thermoplastic composites is their low thermal stability which could potentially be compromised during polymer processing, thus leading to partial CNCs degradation [25].

PHB_{75}/PCL_{25} is a promising biodegradable blend of different thermoplastic polyesters that offers better thermal, impact resistance and elongation properties than the neat PHB, due to the high ductility (high elongation at break values together with low modulus which leads to a rubber-like behaviour) that PCL can provide to this blend. However, PHB_{75}/PCL_{25} shows low miscibility resulting in a phase separation when melt-blended occurs[26], where finely dispersed PCL droplets positively contribute to improve toughness in a similar way as polybutadiene rubber has on toughened styrene-derived polymers such as poly(styrene-co-acrylonitrile) + polybutadiene rubber (ABS) [27]. Despite this, the lack of compatibility between the polymers affects the mechanical properties of the blend, because they are directly related to the ability of its components to transfer stresses [28]. In addition, it is expected that the higher difficulty of degradation of the PCL decreases the biodegradation rate of the blend with respect to the neat PHB [29]. Several studies have corroborated that cellulose nanoparticles could potentially act as

compatibilizers between immiscible polymers through their preferential location among the polymeric interfaces, reducing interface tension which prevents from coalescence of the dispersed phase [30], all this, having a positive effect on the overall properties of composite blends. In this sense, Arrieta *et al.* [31, 32] observed an improvement on interface adhesion between PLA and PHB extruded blends (75/25 wt%) by the addition of 5 wt% of CNCs. The incorporation of CNCs on this PLA/PHB blends enhanced the biodegradation rate, with respect to the unreinforced PLA/PHB blend. The present work aims to study the reinforcing capability of different pine cone CNC loads (3, 5 and 7 wt%), on the performance and disintegration rate of the biodegradable thermoplastic PHB_{75}/PCL_{25} blend. The influence of different CNCs loadings on the mechanical, thermal, morphological, optical and wettability of the PHB_{75}/PCL_{25} blend were studied. The effect of the CNCs on the disintegration rate of the PHB_{75}/PCL_{25} blend has also been compared with the disintegration of the neat PHB. The dispersion of the CNCs in the matrix have been performed by a combination of solvent casting procedure and subsequent manufacturing by extrusion and thermo-compression.

2. EXPERIMENTAL

2.1. Materials

Poly(3-hydroxybutyrate) (PHB) pellets (commercial grade P226) with an average molecular weight of 426 KDa, a density of 1.25 g cm^{-3} and a melt flow index of 10 g·10 min^{-1} (measured at 180 °C with a load of 5 kg) were supplied by Biomer (Krailling, Germany). Poly(ε-caprolactone) (PCL) in pellet form (commercial grade CAPA 6500) with an average molecular weight of 50 KDa was provided by Perstorp Holding AB (Malmö, Sweden). Chloroform ($CHCl_3$, ≥ 99%) was purchased from Sigma Aldrich (Sigma-Aldrich, Germany). Pine cones (*Pinus Pinea*) were collected from a local pine forest in Alicante (Spain)

2.2. Preparation and characteristic of pine cone cellulose nanocrystals

Pine cones were conditioned at 40 ºC for 1 week and then were grinded in a Wiley mill from Thomas Scientific (New Jersey, USA) and subsequently sieved with a 20 μm mesh screen.

Cellulose nanocrystals (CNCs) were isolated from pine cone following the procedure described by Moriana *et al.* [33]. In summary, grinded pine cone particles were subjected to an alkaline and bleaching treatment to remove the amorphous components, such as lignin and hemicellulose. Then, the bleached pine cones were hydrolysed with sulphuric acid (65 wt%) at 45 ºC for 45 min. The obtained suspension was washed with Milli-Q water by using repetitive centrifugations with the following conditions: 10 min at 13.000 rpms and at a temperature of 4 ºC. After this stage, the solution was dialyzed during 7 days with Milli-Q water with the aim of removing the free acid until the wash water reached a constant pH. The resulting CNCs shown a crystallinity index of 88.5%, an onset degradation temperature (T_0) of 150.3 ºC, an average aspect ratio (L/D) of 113.4, an average diameter of 2.9 nm and a percentage cellulose of 97.8% [Daniel Garcia-Garcia, Rafael Balart, Juan Lopez-Martinez, Rosana Moriana, 2018, under review in cellulose journal] Moreover, an ion exchange resin Dowex Marathon MR-3 (hydrogen and hydroxide form) was added to the cellulose suspension for additional 48 h and the removed by filtration with the main aim of ensuring that all ionic moieties were removed except the H+ counter ions associated with the sulphate groups attached to the CNCs surfaces [11]. The resulting suspension was then sonicated using a Sonics Vibra-Cell VCX 750 sonicator from Sonics and Materials Inc. (Connecticut, USA) to promote CNCs dispersion and remove the remaining unhydrolyzed fibers by centrifugation. The final suspension containing CNCs was neutralized by adding NaOH (0.25 mol L^{-1}) until pH of 9 was reached. Finally, a freeze-drying process was carried out to obtain dry CNCs.

2.3. Processing of PHB_{75}/PCL_{25} films with pine cone CNCs

Films of PHB_{75}/PCL_{25} with different CNCs loading (3, 5 and 7 wt%) were prepared by combined melting processing technologies. Table 1 summarized the composition of all the developed materials. The films were obtained by solvent casting, granulated/pelletizated and subsequently subjected to extrusion and thermocompression process. The solvent casting procedure was as follows: the specific amounts of both PHB and PCL were weighed and dissolved in $CHCl_3$ (1 g·25 mL^{-1}) by stirring at 50 ºC for 5 h until full dissolution was achieved; then, the

157 corresponding CNCs loads were dispersed in $CHCl_3$ by using a Sonics Vibra-Cell VCX 750
158 sonicator for 20 min (5 x 4 min) in an ice bath; after that, the dispersed CNCs were mixed together
159 with the PHB_{75}/PCL_{25} solution in $CHCl_3$ and the mixtures were vigorously stirred for 1 h; and,
160 finally, the mixture was maintained at room temperature until $CHCl_3$ was completely evaporated,
161 followed by oven vacuum drying at 40 ºC overnight.
162
163 **Table 1.** Composition and codes for poly(3-hydroxybutyrate)/poly(ε-caprolactone) (PHB/PCL)
164 blend films with pine cone cellulose nanocrystals (CNCs).

Coding	PHB (wt%)	PCL (wt%)	CNC (wt%)
PHB	100	0	0
PHB_{75}/PCL_{25}	75	25	0
3% CNC	72.75	24.25	3
5% CNC	71.25	23.75	5
7% CNC	69.75	23.25	7

165
166 To increase the CNCs dispersion in the PHB_{75}/PCL_{25}, the solvent casting films were
167 reduced until reaching pieces of about 3 mm and subjected to a compounding process in a DSM
168 Xplore Micro 5cc twin screw microextruder from Xplore Instruments BV (Sittard, The
169 Netherlands) at 180 ºC. The screw speed was set to 120 rpm and the mixing time did not exceed
170 3 min to avoid thermal degradation of PHB and CNCs. Then, the material was discharged and
171 cooled at room temperature, pelletized and vacuum dried at 40 ºC overnight. Finally, the dry
172 compounded material was compression molded to 100 μm films using a hot press Fontijne model
173 TP400 (Barendrecht, The Netherlands). The material was preheated up to 180 ºC for 1 min and
174 then, subjected to a pressure of 200 MPa for 1 additional min. After this, the obtained materials
175 were cooled down to room temperature by maintaining the compaction pressure.
176
177 **2.4. Characterization techniques**
178 *2.4.1. UV–vis spectrometry*

The light transmission properties of the PHB_{75}/PCL_{25} films with the different CNCs loads, were measured in the 250−700 nm wavelength range with a Shimadzu UV-2550 UV-Vis spectrophotometer from Shimadzu Scientific Instruments (Columbia, USA). The software UVProbe 2.0 was used to obtain and analyze the data. The measurements were done in triplicate and the average of the three spectra was obtained.

2.4.2. Static contact angle measurements

The static contact angle of neat PHB and PHB_{75}/PCL_{25} films with different CNCs loadings was obtained using a CAM 200 goniometer from KSV Instruments (Helsinki, Finland) equipped with a Basler A602f camera. The liquid for the contact angle measurement was Milli-Q water and the volume of the droplets was 5 μL. Prior to contact angle measurements, all samples were conditioned at 23 ºC and 50% RH for 48 h. The static water contact angle was obtained using the CAM200 software applying the Young-Laplace fitting method. All contact angles were taken 5 s after the droplet was dropped into the film surface. At least, five different measurements for each film were obtained and averaged.

2.4.3. Field emission scanning electron microscopy (FESEM)

Cross section of nitrogen cryofractured films was investigated in a field emission scanning electron microscope (FSEM) ZEISS Ultra55 from Oxford Instruments (Oxforshire, United Kingdom) working at an acceleration voltage of 2 kV. With the aim of providing electrical conductivity to the polymeric samples, the fracture surfaces were coated with a thin layer of platinum in a high vacuum sputter coater EM MED20 from Leica Microsystems (Wetzlar, Germany).

2.4.4. Mechanical properties

Tensile tests on films were carried out with an Instron 5944 machine from Instron Ltd. (Norwood, USA) using a 500 N load cell. Film samples with dimensions of 50 x 5 mm^2 were subjected to an initial gauge length of 25 mm and then, a crosshead speed was 2 mm min^{-1} was

applied to obtain the main tensile parameters: tensile modulus (E_t), tensile strength (σ_t) and elongation at break (ε_b). The thickness of the films was accurately measured with a Mitutoyo micrometer by taking the average thickness of five different areas of each film. All the films were subjected to a conditioning stage at 23 ± 1 °C and 50% RH for 48 h prior to testing. Five different replicates of each sample were tested and the average values of the above-mentioned tensile properties were calculated.

2.4.5. Thermal properties

Thermal properties of the films were obtained by means of Thermogravimetric analysis (TGA) and Differential Scanning Calorimetry (DSC). TGA was conducted in a Mettler-Toledo TGA/DSC 1 thermobalance (Schwerzenbach, Switzerland) under nitrogen atmosphere (the flow rate was set to 50 mL min^{-1}). The films were cut into small pieces (5−6 mg) and were taken and placed into standard alumina crucibles. A dynamic heating program from 30 ºC to 750 ºC at a heating rate of 10 ºC min^{-1} was applied. The onset degradation temperature (T_0) was assumed as the temperature at which, a weight loss of 5% with regard the initial mass, occurs. The maximum degradation rate temperature (T_{max}) for each degradation stage was located at the corresponding peak in the first derivative curve (DTG). DSC measurements were obtained in a Mettler-Toledo DSC 822e calorimeter (Schwerzenbach, Switzerland). The tests were run under nitrogen atmosphere with a flow rate of 50 mL min^{-1}. In a similar way to sample preparation for TGA, the films were cut into small pieces and, approximately 4 mg were placed in standard aluminium crucibles (40 µL). The thermal program was as follows: a first heating stage from -50 ºC to 180 ºC was applied to remove the thermal history; then, an isothermal stage at 180 ºC for 1 min was scheduled. After this, a cooling process down to -50 ºC was programmed and, finally, a second heating stage from -50 ºC up to 300 ºC was applied. The heating/cooling rate for all stages was set to 10 ºC min^{-1}. All DSC tests were run in triplicate to obtain reliable results. The melt peak temperature (T_m) was taken from the second heating stage and the degree of crystallinity (X_c) of both PHB and PCL was calculated by following this equation:

$$X_c\,(\%) = 100 \times \left[\frac{\Delta H_m}{\Delta H_0 \cdot w}\right] \qquad \text{Equation 1}$$

Where ΔH_m stands for the thermodynamic melt enthalpy per gram, ΔH_0 represents the theoretical melt enthalpy associated to the corresponding 100% crystalline polymer (these values were assumed to be 146 J g^{-1} [34] for PHB and 156.8 J g^{-1} [35] for PCL), and *w* is the weight fraction of the corresponding polymer (PHB or PCL) in the blend.

2.4.6. Fourier transformed infrared spectroscopy (FTIR)

FTIR spectra of PHB and PHB_{75}/PCL_{25} films with different CNCs content were obtained at room temperature on a Perkin-Elmer Spectrum 2000 FTIR instrument (Waltham, USA) equipped with a single reflection attenuated total reflectance (ATR) accessory unit, with a diamond ATR crystal Golden Gate from Specac Ltd. (Kent, England). Each spectrum was acquired in the wavelength range of 600−4000 cm^{-1} from 16 scans with a resolution of 4 cm^{-1}. All spectra were fitted to an automatic base line correction and normalized using the Perkin-Elmer software Spectrum.

2.3.7. X-ray diffraction spectroscopy (XRD)

X-ray diffraction (XRD) characterization of PHB and PHB_{75}/PCL_{25} of films was carried out using an X-ray diffraction on a Bruker CCD-Appex apparatus equipped with an X-ray generator (Ni filtered Cu-Kα radiation) operated at 40 kV and 40 mA. The samples were scanned from 5º to 40º (2θ) at a scanning rate of 2º min^{-1}.

2.4.8. Disintegration under composting conditions

The degradation rate under controlled compost soil of PHB and PHB_{75}/PCL_{25} blend with different CNCs content was carried out as indicated by ISO20200. Films were cut into squared shapes (25x25 mm^2) with an average thickness of 100 μm. Initially, samples were dried overnight at 40 ºC, weighed and subsequently, were buried at a depth of 4−6 cm in a plastic reactor

containing a solid synthetic wet soil prepared with 40 wt% sawdust, 30 wt% rabbit-feed, 10 wt% corn starch, 10 wt% compost, 5 wt% sugar, 4 wt% corn oil and 1 wt% urea. Finally, distilled water was added to the synthetic solid waste to a 45:55 ratio. Samples were subjected to an aerobic degradation (disintegration) at a constant temperature of 50 ºC in an air-circulating oven for a total time of 70 days. Periodically, as recommended by the standard, samples were extracted from the reactor, washed with distilled water, dried at 40±2 ºC for 24 h and, finally, weighed at different testing times to follow the weight evolution during the disintegration process.

3. RESULTS AND DISCUSSION

3.1. Optical properties

Figure 1a shows the visual appearance of the obtained films over a picture to see their transparency. All the developed films show high transparency as the lower logo can be clearly seen. Visually, there are not significant differences between the loaded or unloaded films; only, a slight change to dark tones can be detected in films as the CNCs content increases. UV-vis characterization was carried out to evaluate the light transmission of the films in the wavelength range comprised between 250 – 700 nm. Figure 1b shows the light transmission spectra corresponding to films of PHB_{75}/PCL_{25} blend with varying CNC content. As can be seen, the blend PHB_{75}/PCL_{25} shows the lowest transmittance value at 700 nm (2,8%) which is directly relate to lower transparency. Nevertheless, after the addition of CNCs to the PHB_{75}/PCL_{25} blend, the transmittance is noticeably improved, being the films with 3 wt% CNCs the ones that show the highest transmittance (17.8%). This noticeable increment in the transmittance could be related to a good CNCs dispersion and a good CNC/matrix interaction in the 3% CNC films. Seoane *et al.* [36] and Chen *et al.* [37] confirmed how these two phenomena contribute to lower light dispersion and, consequently, enhancing the light transmission thorough the film. On the other hand, the lower transmittance of the 5%CNC and 7%CNC films may be due to formation of CNCs aggregates which contributes to poor dispersion and, subsequently, the optical properties get worse [38]. However, the transmittance values in the UV-Vis region for all the films are lower than 5%, giving evidence of the good UV barrier properties in comparison to other bio-based

polyesters such as PLA [39]. The UV protection that the herein developed formulations offer, together with the high transparency after addition of 3 wt% CNC, could represent interesting features for the food-packaging industry which requires both properties: on one hand, food protection against light and, on the other hand, good transparency to see the packaging content [40].

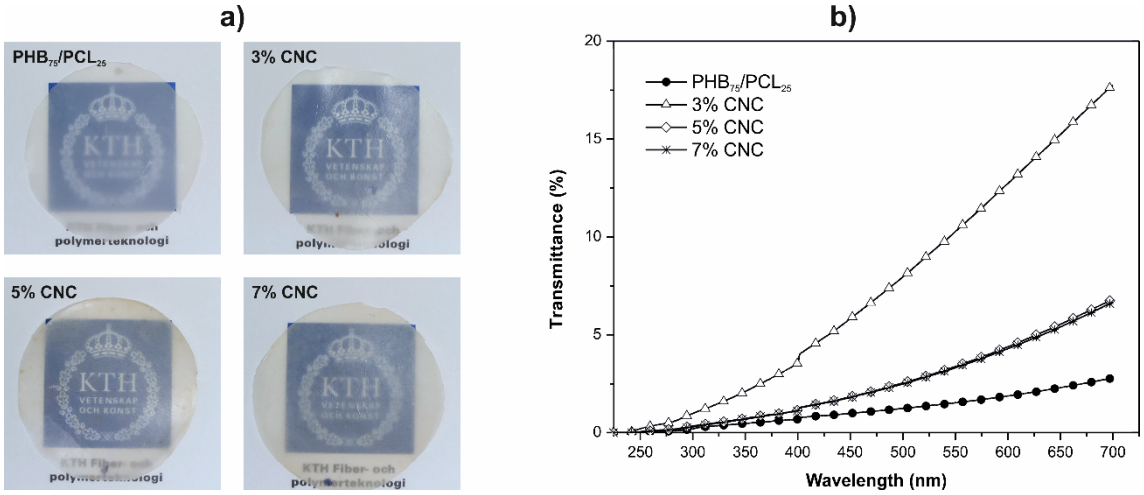

Figure 1. a) Visual appearance and b) UV-vis spectra of PHB_{75}/PCL_{25} films with different CNCs content.

3.2. Wettability

The water contact angle values of films were obtained to assess the wetting behaviour of the different developed films. Figure 2 shows a bar plot of the static water contact angle (θ_w) for all the developed films. As suggested by Vogler [41] θ_w values lower than 65º are representative for a hydrophilic behaviour while θ_w values over 65 ºC stand for hydrophobic surfaces. PHB_{75}/PCL_{25} , shows higher values of θ_w (80º) due to the high hydrophobic nature of PCL [42]. The addition of CNCs in the PHB_{75}/PCL_{25} films provides a progressive decrease in its surface hydrophobicity as a function of the CNCs increment. This is evidenced by a decrease in θ_w down to values of 72.3º for 7% CNC films, and it is directly related to an increase in the hydroxyl groups that CNCs provide to films [43]. As it can be outlined, addition of CNCs to the PHB_{75}/PCL_{25} film does not affect in a remarkable way to its hydrophobic nature. This is an important feature for

food-packaging industry where food protection against moisture is needed during transportation and storage [32].

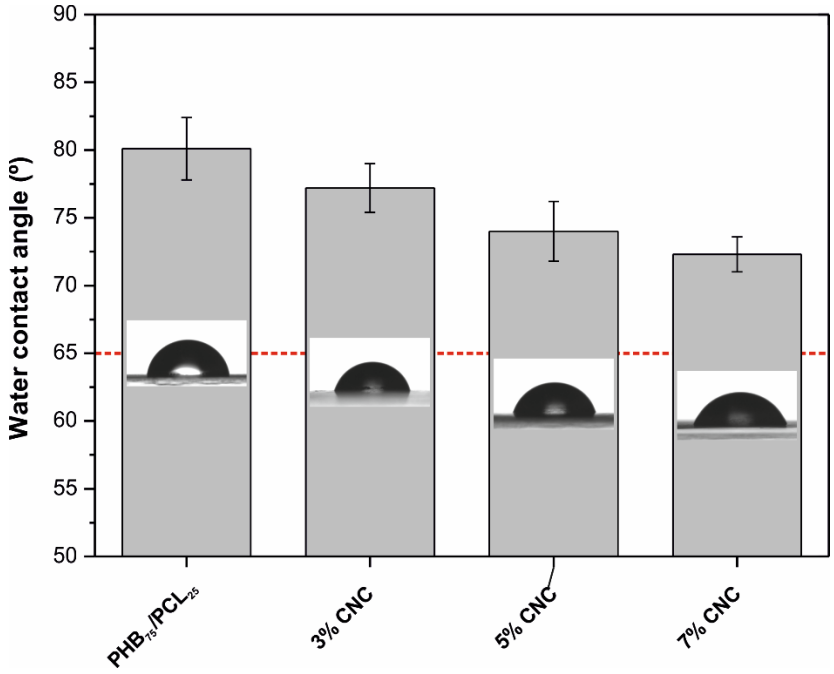

Figure 2. Contact angle measurement of PHB_{75}/PCL_{25} films with different CNCs content.

3.3. Morphological properties

Field emission scanning electron microscopy (FESEM) of PHB_{75}/PCL_{25} films with different CNC loadings was carried out on the cross-section of films to evaluate the morphology and analyze CNC dispersion in the polymer matrix (Figure 3). The fracture of the PHB_{75}/PCL_{25} blend (Figure 3a) shows a typical droplet structure, specifically, spherical PCL-rich particles can be clearly distinguishable as a randomly dispersed droplet-like phase, indicating both polymers are immiscible [26]. On the other hand, 3% CNCs films show a homogeneous dispersion without aggregates indicating the presence of CNCs enhances the compatibility between the immiscible polymers, reducing the phase separation which may contribute to improved mechanical properties. The films with higher CNCs loading (5 and 7 wt%) display an increase in surface roughness with irregular protrusions and holes, which are typical of CNC aggregate formation. These aggregates can be observed in the fracture surface in the Figure 3c and Figure 3d. This may

corroborate that higher CNCs amounts in the PHB_{75}/PCL_{25} blend leads to aggregate CNCs formation, thus leading to a poor particle dispersion. These aggregates contribute to a lack of continuity into the matrix, which may have a negative effect on stress transfer.

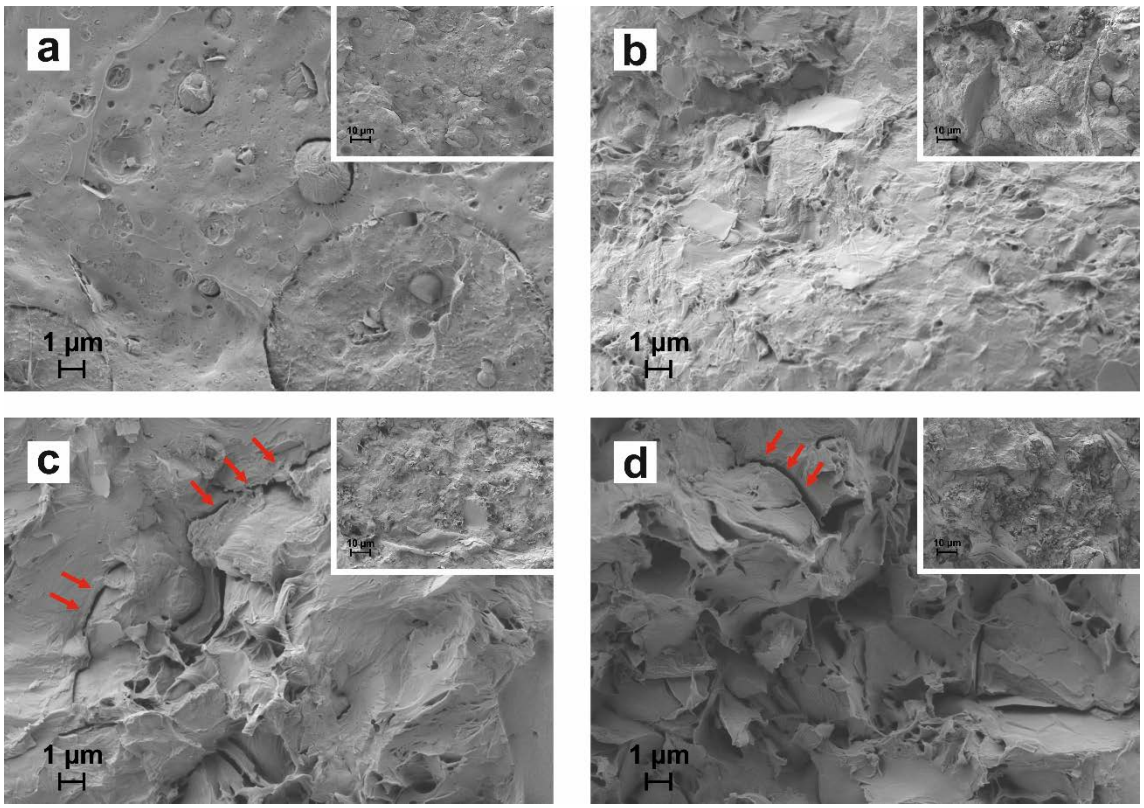

Figure 3. Field emission scanning electron microscopy (FESEM) images of fracture surface of (a) PHB_{75}/PCL_{25}; (b) 3% CNC; (c) 5% CNC; and, (d) 7% CNC.

3.4. Mechanical properties

The mechanical properties of the developed films with different CNCs loading are compared with those obtained for the PHB_{75}/PCL_{25} blend (Table 3). The PHB_{75}/PCL_{25} blend has a tensile strength of 14.7 MPa, a Young's modulus of 949 MPa and an elongation at break close to 4%. These mechanical properties remain similar with the addition of 3 wt% CNCs. However, a significant reduction in the standard deviation of all parameters can be observed, which could be related to a good CNCs dispersion which gives increased interface adhesion and, subsequently, leads to more homogenous interactions between PHB and PCL. Over this load percentage, both

the tensile strength and elongation at break significantly decreases, whereas the young modulus increases with regard to the PHB_{75}/PCL_{25} blend. Therefore, the addition of 5% and 7% CNCs in the PHB_{75}/PCL_{25} resulted in a more fragile and stiffer film due to the presence of CNC aggregates. This poor dispersion of the CNCs on the blend leads to a lack of continuity in the matrix with the subsequent embrittlement and stress concentration phenomena [44].

Table 3. Tensile properties of PHB_{75}/PCL_{25} blends with different CNCs content.

Sample	Tensile Strength (MPa)	Young's modulus (GPa)	Elongation at break (%)
PHB/PCL	14.7 ± 1.3	949 ± 90	3.9 ± 0.7
3% CNC	14.5 ± 0.7	902 ± 56	4.1 ± 0.4
5% CNC	9.3 ± 1.4	1066 ± 65	1.8 ± 0.9
7% CNC	6.5 ± 1.7	972 ± 96	0.4 ± 1.1

3.5. Thermal properties

The effect of CNCs addition on the thermal stability PHB_{75}/PCL_{25} blends were studied by thermogravimetric analysis. Figure 4 shows the thermogravimetric (TG) and first derivative (DTG) curves for all the studied materials. PHB_{75}/PCL_{25} blend is characterized by an onset degradation temperature (T_0) of 249.5 ºC and displays two degradation stages: the first weight loss is directly related to PHB with a maximum degradation rate (T_{max}) of 233.5 ºC; and the second stage is mainly attributable to PCL degradation which a maximum degradation rate (T_{max}) of 249.5 ºC [28]. Addition of CNCs to the PHB_{75}/PCL_{25} blend leads to a decrease in the thermal stability (Table 4). Specifically, the onset degradation for the films moves to lower values (229.5, 224.0 and 221.0 ºC for the blends containing 3, 5 and 7 wt% CNCs) that are more similar to the PHB onset [26]. Moreover, a decrease in the maximum degradation rate (T_{max}) related to the PHB and PCL in the PHB_{75}/PCL_{25} blend also occurs as a function of the CNCs content. This phenomenon is related to the lower thermal stability of CNCs with a maximum degradation rate located around 308 ºC. Despite this low thermal stability of CNCs, all reinforced blends showed enough thermal stability during the different manufacturing stages.

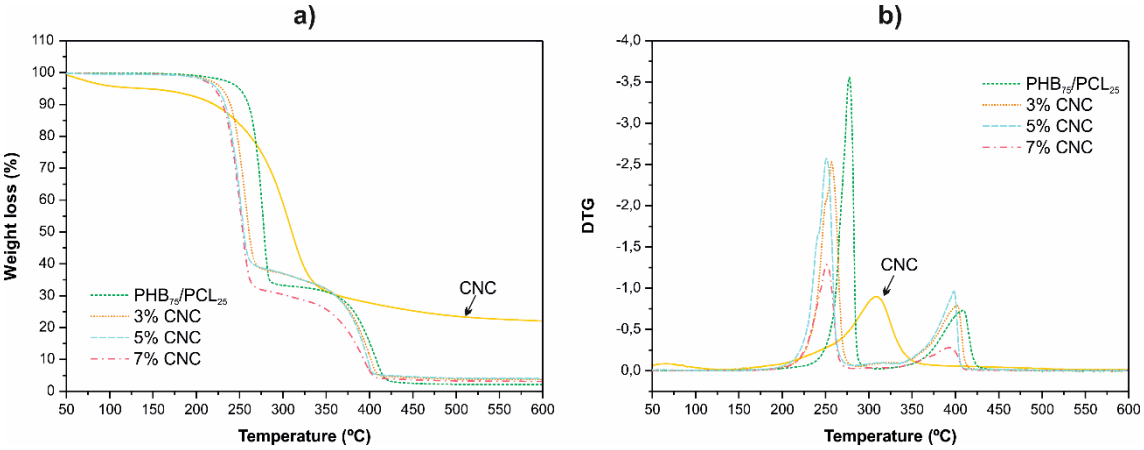

Figure 4. Thermal degradation of PHB_{75}/PCL_{25} films with different CNCs content, (a) TG weight loss and (b) first derivative DTG curves.

The effects of CNCs on the crystalline phase (melting and crystallization) of the thermoplastic blends (PHB_{75}/PCL_{25}) was followed by differential scanning calorimetry (DSC). DSC curves corresponding to the second heating cycle (after removing thermal history) of all the developed materials are gathered in Figure 5. The main thermal parameters obtained by DSC are summarized in Table 3. Due to the high immiscibility between PHB and PCL, the melting processes of both polymers can be clearly seen in Figure 5. The melt peak temperature for PCL is located at 54.7 ºC while the melt peak temperature for PHB is around 169.5 ºC [26]. After addition of CNCs to the PHB_{75}/PCL_{25} blend, important changes in the thermal transitions can be observed. The peak related to the melting of PHB splits, leading to the formation of two peaks. This effect could be due to the heterogeneous nucleating effect of CNCs on PHB which, give rise to the development of PHB small crystals with different morphology compared to typical PHB crystals [45, 46]. Therefore, the presence of multiple PHB melting peaks may be related to the formation of a different crystal structures [47]. The melt peak temperature and crystallinity decreases with increasing CNCs content in the films, indicating imperfect crystals leads an easier and faster melting of the PHB as the content of CNCs increases [48]. According to Yu et al. [46] CNCs may modify chain diffusion and folding during polyester spherulitic growth due to hydrogen bonding interactions between CNCs and polyester matrix, resulting in a decrease of

crystallinity. Therefore, the larger CNCs content in the films could provoke larger number of hydrogen bonding interactions and lower crystallinity. On the other hand, CNCs do not affect in a remarkable way to the PCL crystallinity as previously reported by Mi *et al.* [8].

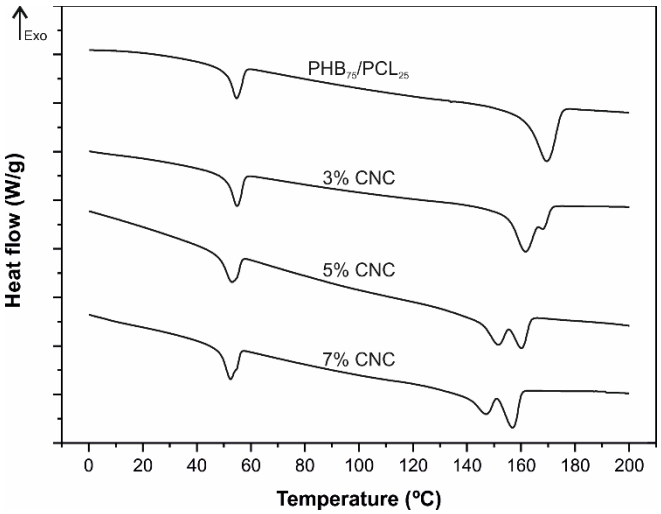

Figure 5. DSC thermograms of the second heating cycle of PHB_{75}/PCL_{25} blend with different CNCs content.

Table 4. Main thermal parameters of neat PHB and PHB_{75}/PCL_{25} blend with different CNCs content.

Samples	DSC Parameters						TGA Parameters		
	$T_{m\ PCL}$ (ºC)	$\Delta H_{m\ PCL}$ (J g^{-1})	$X_{c\ PCL}$ (%)	$T_{m\ PHB}$ (ºC)	$\Delta H_{m\ PHB}$ (J g^{-1})	$X_{c\ PHB}$ (%)	T_0[a] (ºC)	$T_{max\ PHB}$ (ºC)	$T_{max\ PCL}$ (ºC)
PHB	-	-	-	167.4	-74.8	51.3	233.5	267.0	-
PHB/PCL	54.7	-67.8	43.2	169.5	-67.3	46.1	249.5	277.5	409.5
3% CNC	54.8	-65.2	41.6	161.7/168.0	-66.8	45.7	229.5	257.0	401.5
5% CNC	53.0	-66.3	42.3	151.7/160.1	-59.9	41.0	224.0	251.0	398.0
7% CNC	52.4	-68.0	43.4	147.1/156.8	-55.7	38.2	221.0	251.0	393.0

[a] T_0, calculated at 5% mass loss.

3.6. Chemical structural properties

The infrared spectra of PHB_{75}/PCL_{25} blend and its films with different CNCs loads are gathered in Figure 6. The PHB_{75}/PCL_{25} spectrum shows the characteristic bands of both PHB and PCL: the broad band at 3000-2900 cm^{-1} which is assigned to $–CH_3$, asymmetric $–CH_2–$, and $–CH_2–$ symmetric stretching vibrations [6]; the peak located at 1720 cm^{-1} which is directly related to the ester carbonyl C=O [49]; the peak located at 1280 cm^{-1} which is attributed to C−O stretching [50]; the peak around 1165 cm^{-1} which is attributed to C-O-C stretching [42]. After CNC addition to the PHB_{75}/PCL_{25} blend, an increase in the intensity of the hydroxyl absorption band (3400 – 3200 cm^{-1}), specifically is clearly detected as a function of the CNCs loading [32]. It is also possible to observe an increase in the peak intensity at 2940 cm^{-1} which is related to the >CH- vibration contribution of CNCs [51]. Two additional peaks at 1420 cm^{-1} and 1370 cm^{-1} can be clearly identified in the FTIR spectra of PHB_{75}/PCL_{25} blends with the different CNCs load. The first one, located at 1420 cm^{-1} is related with the bending vibration mode of hydroxyl group [51] while the other one, around 1370 cm^{-1} stands fort the –C–H bending from the crystalline region of cellulose [49].

The effect of CNCs on the decrease in the PHB crystallinity can be detected by FTIR as the typical peaks/bands of the crystalline PHB regions (980, 1228, 1276 and 1720 cm^{-1}) are less intense [49, 52]. On the other hand, the intensity of the peak located at 1740 cm^{-1}, related to carbonyl groups in PHB amorphous regions, is more intense and therefore the carbonyl region become broader with the addition of CNCs (Figure 6b). These results proved the formation of hydrogen bonding interactions between OH groups of CNCs and C=O groups of PHB_{75}/PCL_{25} blends [53]. These hydrogen bonding interactions may hinder the diffusion rate and folding of crystalline polyester chains, resulting in a slight decrease of crystallinity [46]. Therefore, the CNCs addition on the PHB_{75}/PCL_{25} decreases the PHB crystallinity values as shown in DSC analysis.

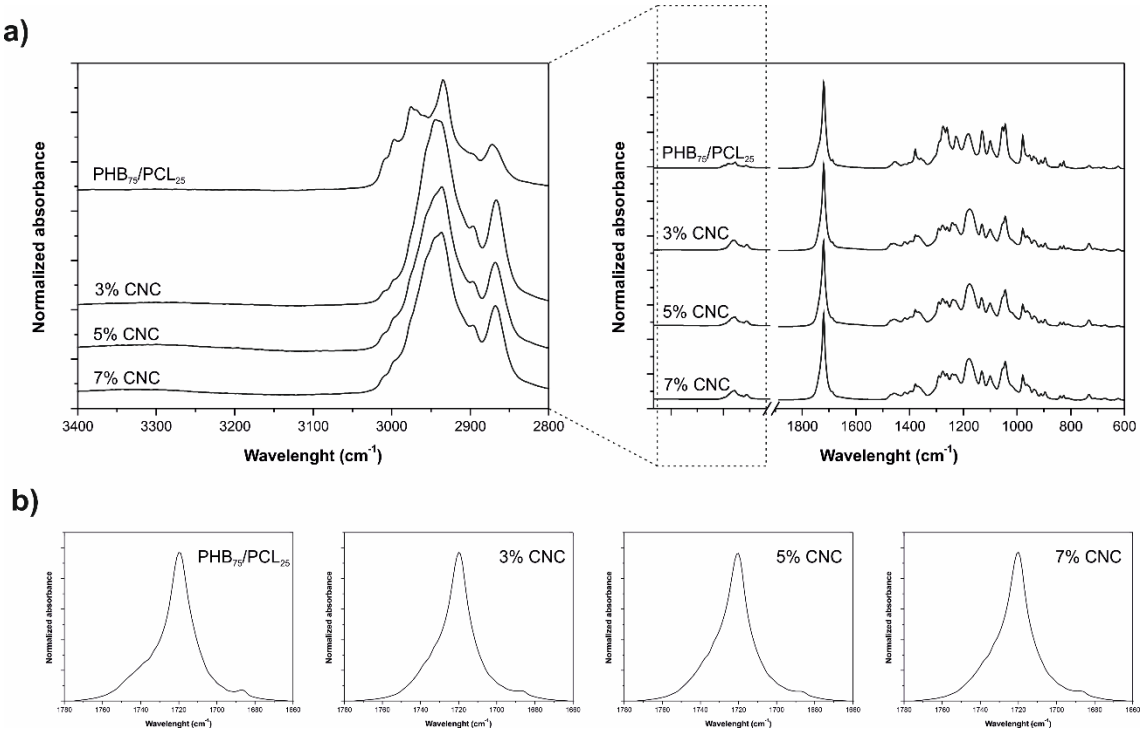

Figure 6. (a) FTIR spectra diffraction patterns of PHB_{75}/PCL_{25} blend with different CNCs content. (b) FTIR spectra magnification in the wavelength between 1660 and 1780 cm^{-1}.

Figure 7 shows the XRD diffractograms of PHB_{75}/PCL_{25} blends with different CNC loads and compared them with the un-reinforced PHB_{75}/PCL_{25} blend. The PHB_{75}/PCL_{25} blend shows the characteristic peaks of both polymers. A typical XRD diffractogram of PHB shows a series of characteristic crystallinity peaks at 2θ= 13.5º, 16.9º, 20.1º, 21.4º 22.5º, 25.1º and 28.6º which correspond to the reflection planes (020), (110), (021), (101), (121), (040) and (002) characteristics of the orthorhombic unit cell of PHB [53-55]. On the other hand, the typical XRD peaks of PCL are located at 2θ = 21.4º and 2θ = 23.7º. These two peaks are directly related to the main reflection planes of PCL, namely the plane (110) and (200), typical of the orthorhombic unit cell of PCL [54, 56]. In general, after the addition of CNCs, no significant changes can be detected, being all the XRD spectra similar to those of the PHB_{75}/PCL_{25} blend. Despite this, a slight decrease in the intensity of the typical diffraction peaks corresponding to planes (020), (110) and (002) of PHB crystals can be detected which is representative for the slight decrease in crystallinity suggested by both DSC analysis and FTIR characterization. CNCs also affect the

crystal structure of the base polymers in the blend. It is possible to detect an increase in the intensity of the peak located at 2θ = 22.5 (clearly distinguishable for composites with 7 wt% CNCs) as this peak is characteristic of the diffraction pattern of cellulose [57].

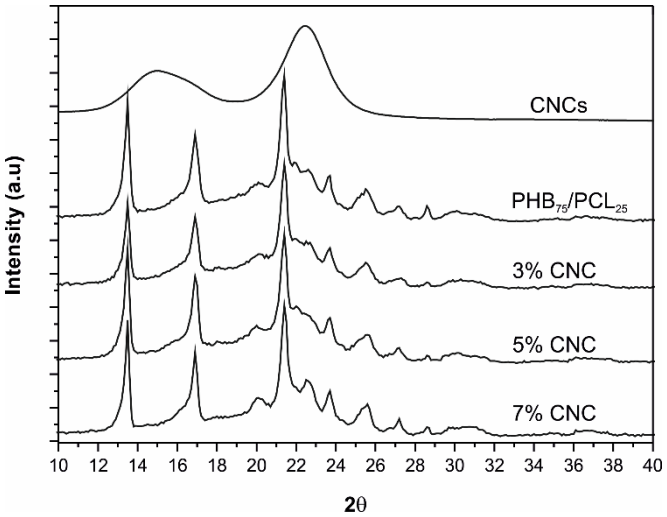

Figure 7. X-ray diffraction patterns of PHB_{75}/PCL_{25} blend with different CNCs content.

3.7. Disintegration under composting

The visual appearance of neat PHB and the PHB_{75}/PCL_{25} blend with different CNCs loads during the disintegration test in controlled compost soil can be seen in Figure 8a. Figure 8b shows in a quantitative way the weight loss evolution during the disintegration test in terms of incubation/disintegration time. The line at 90% weight loss, stands for the goal of disintegrability as indicated in the corresponding standard [32]. It is possible to conclude that all the developed materials, start losing mass after the first day. The disintegration rate of neat PHB has been also studied with the aim of evaluating the influence of the PCL on the biodegradability of the PHB. As can be seen, neat PHB offers the highest weight loss during the first 10 incubation days; nevertheless, it becomes highly brittle after 28 days incubation time and reaching 90% weight loss at 53 days. PCL is more resistant to disintegration than PHB. For this reason, PHB_{75}/PCL_{25} blend show increased degradation time. Specifically, this blend becomes highly brittle for an incubation time of 49 days while a 90% weight loss is reached after 67 days which represents a degradation time two weeks later than neat PHB. This is attributable to the lower disintegration

rate of PCL compared to PHB [29]. CNCs have a positive effect on enhancing disintegration. In fact, all the films with CNCs become highly brittle (see Figure 8a) at about 14 days and a disintegration level of 90% is reached after 47, 41 and 40 days for blends containing 3, 5 and 7 wt% CNCs respectively. This increment in the degradation rate could be related to the hydrophilicity of the PHB_{75}/PCL_{25} blend after the addition of CNCs as it was previously observed by contact angle measurements (Figure 2a). This hydrophilicity provided by CNCs favour disintegration of PHB by an hydrolysis process in which, high molecular PHB chains hydrolyse to form low molecular weight chains [58]. On the other hand, the decrease in the disintegration time in all blends with CNCs is also affected by the crystallinity degree since crystalline regions are more resistant to hydrolysis [40]. In accordance with the change in crystallinity observed by DSC, FTIR and XRD, presence of CNCs contributes to reduce the crystalline regions in the thermoplastic blend and this has a positive effect on enhancing the disintegration rate.

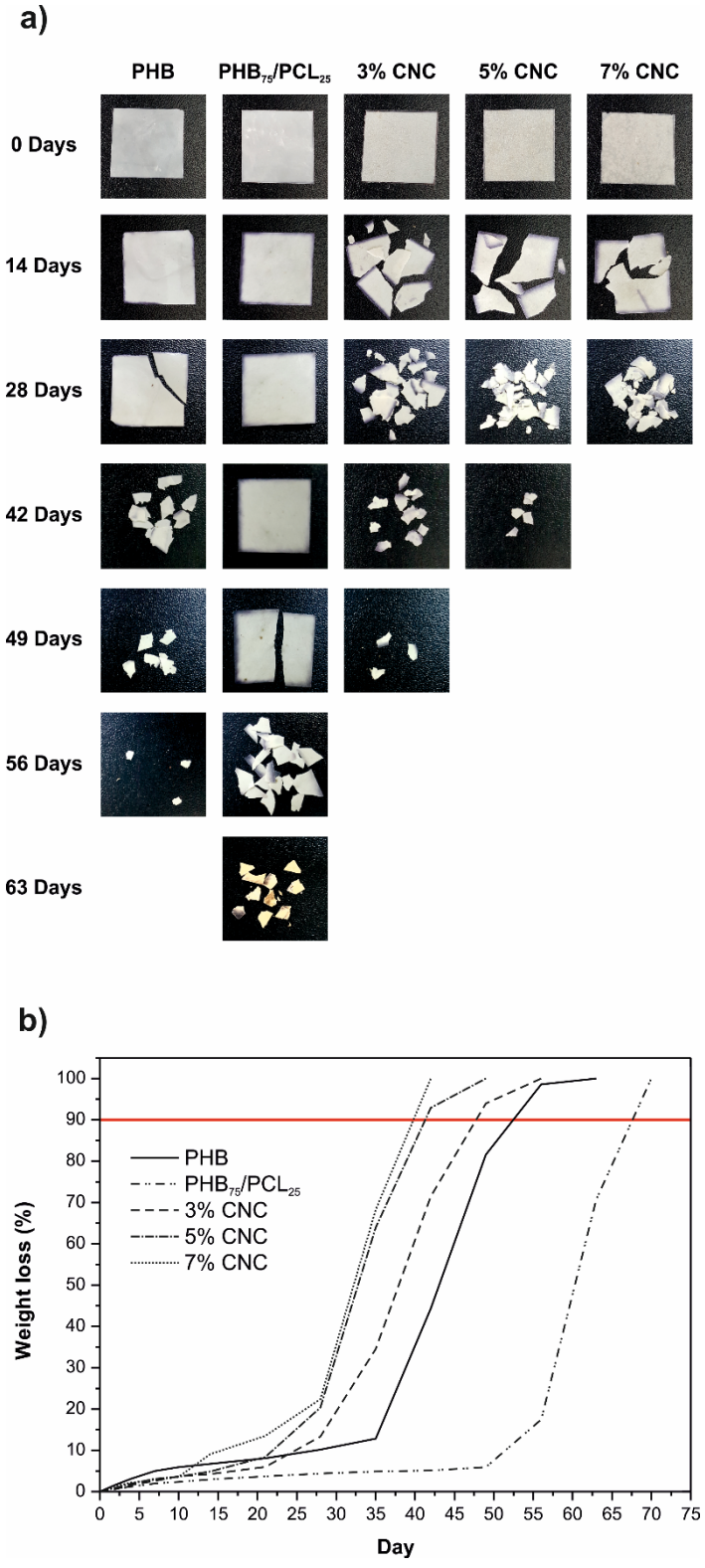

Figure 8. Evolution of the disintegration in controlled compost soil in terms of the incubation time of neat PHB and PHB_{75}/PCL_{25} blends with different CNCs load, a) qualitative visual appearance of the aged films and (b) weight loss during the disintegration process on aged films.

CONCLUSIONS

Different amounts of cellulose nanocrystals (3, 5 and 7 wt%) obtained from Pine Cone by acid hydrolysis were successfully incorporated into PHB / PCL blends (75/25) by solvent casting followed by extrusion and thermocompression. In the present work the reinforcing capability of different amounts of CNCs on the mechanical, thermal, chemical, morphological, optical and wettability properties of PHB_{75}/PCL_{25} blends has been studied. The incorporation of low quantities of CNCs (3 wt%) to the blend of PHB_{75}/PCL_{25} gives a good dispersion and improves the interfacial adhesion between both polymers, considerably improving the transparency of the film without affecting the mechanical properties. Higher amounts of CNCs (5 and 7 wt%) tend to form aggregates, resulting in a loss of transparency and poorer mechanical properties that the unreinforced PHB_{75}/PCL_{25} blend. The incorporation of CNCs in the blend also causes an increase in wettability, due to the hydrophilic character. The disintegration test demonstrated that the incorporation of CNCs to PHB_{75}/PCL_{25} blend accelerates considerably the disintegration process with respect to the unreinforced blend, obtaining a faster disintegration as the content of CNC increases. The results obtained show how the best balance between mechanical, thermal, optical and disintegration rate properties is obtained after the incorporation of a 3 wt% CNCs.

Some of the results obtained in the present work, such as the high transparency level and the high degradation rate of PHB/PCL films after addition of 3 wt% CNC, together with a high hydrophobicity, good UV barrier properties and balanced mechanical properties, give interesting applications to these materials in the food-packaging industry.

ACKNOWLEDGEMENTS

This research was supported by the Ministry of Economy and Competitiveness – MINECO through the gran number MAT2014-59242-C2-1-R. D. Garcia-Garcia wants to thank

509 the Spanish Ministry of Education, Culture and Sports for the financial support through a FPU
510 grant number FPU13/06011.

REFERENCES

[1] M.M. Haafiz, A. Hassan, Z. Zakaria, I.M. Inuwa, M.S. Islam, M. Jawaid, Properties of polylactic acid composites reinforced with oil palm biomass microcrystalline cellulose, Carbohydrate polymers 98(1) (2013) 139-145.

[2] H.-Y. Yu, Z.-Y. Qin, C.-F. Yan, J.-M. Yao, Green nanocomposites based on functionalized cellulose nanocrystals: a study on the relationship between interfacial interaction and property enhancement, ACS Sustainable Chemistry & Engineering 2(4) (2014) 875-886.

[3] E. Fortunati, M. Peltzer, I. Armentano, L. Torre, A. Jiménez, J. Kenny, Effects of modified cellulose nanocrystals on the barrier and migration properties of PLA nano-biocomposites, Carbohydrate polymers 90(2) (2012) 948-956.

[4] C. Zhou, Q. Shi, W. Guo, L. Terrell, A.T. Qureshi, D.J. Hayes, Q. Wu, Electrospun bio-nanocomposite scaffolds for bone tissue engineering by cellulose nanocrystals reinforcing maleic anhydride grafted PLA, ACS applied materials & interfaces 5(9) (2013) 3847-3854.

[5] E. Fortunati, F. Luzi, D. Puglia, F. Dominici, C. Santulli, J. Kenny, L. Torre, Investigation of thermo-mechanical, chemical and degradative properties of PLA-limonene films reinforced with cellulose nanocrystals extracted from Phormium tenax leaves, European Polymer Journal 56 (2014) 77-91.

[6] P. S de O Patrício, F.V. Pereira, M.C. dos Santos, P.P. de Souza, J.P. Roa, R.L. Orefice, Increasing the elongation at break of polyhydroxybutyrate biopolymer: Effect of cellulose nanowhiskers on mechanical and thermal properties, Journal of Applied Polymer Science 127(5) (2013) 3613-3621.

[7] A.-L. Goffin, J.-M. Raquez, E. Duquesne, G. Siqueira, Y. Habibi, A. Dufresne, P. Dubois, Poly (ε-caprolactone) based nanocomposites reinforced by surface-grafted cellulose nanowhiskers via extrusion processing: morphology, rheology, and thermo-mechanical properties, Polymer 52(7) (2011) 1532-1538.

[8] H.-Y. Mi, X. Jing, J. Peng, M.R. Salick, X.-F. Peng, L.-S. Turng, Poly (ε-caprolactone)(PCL)/cellulose nano-crystal (CNC) nanocomposites and foams, Cellulose 21(4) (2014) 2727-2741.

[9] I. Pinheiro, F. Ferreira, D. Souza, R. Gouveia, L. Lona, A. Morales, L. Mei, Mechanical, rheological and degradation properties of PBAT nanocomposites reinforced by functionalized cellulose nanocrystals, European Polymer Journal 97 (2017) 356-365.

[10] N. Bitinis, R. Verdejo, J. Bras, E. Fortunati, J.M. Kenny, L. Torre, M.A. López-Manchado, Poly (lactic acid)/natural rubber/cellulose nanocrystal bionanocomposites Part I. Processing and morphology, Carbohydrate polymers 96(2) (2013) 611-620.

[11] E. Fortunati, I. Armentano, Q. Zhou, A. Iannoni, E. Saino, L. Visai, L.A. Berglund, J. Kenny, Multifunctional bionanocomposite films of poly (lactic acid), cellulose nanocrystals and silver nanoparticles, Carbohydrate polymers 87(2) (2012) 1596-1605.

[12] N. Soykeabkaew, N. Tawichai, C. Thanomsilp, O. Suwantong, Nanocellulose-Reinforced "Green" Composite Materials, Walailak Journal of Science and Technology (WJST) 14(5) (2016) 353-368.

[13] H.-M. Ng, L.T. Sin, T.-T. Tee, S.-T. Bee, D. Hui, C.-Y. Low, A. Rahmat, Extraction of cellulose nanocrystals from plant sources for application as reinforcing agent in polymers, Composites Part B: Engineering 75 (2015) 176-200.

[14] Y. Habibi, L.A. Lucia, O.J. Rojas, Cellulose nanocrystals: chemistry, self-assembly, and applications, Chem. Rev 110(6) (2010) 3479-3500.

[15] A. Pei, Q. Zhou, L.A. Berglund, Functionalized cellulose nanocrystals as biobased nucleation agents in poly (l-lactide)(PLLA)–Crystallization and mechanical property effects, Composites Science and Technology 70(5) (2010) 815-821.

[16] R. Moriana, F. Vilaplana, M. Ek, Cellulose nanocrystals from forest residues as reinforcing agents for composites: A study from macro-to nano-dimensions, Carbohydrate polymers 139 (2016) 139-149.

[17] M. Le Normand, R. Moriana, M. Ek, Isolation and characterization of cellulose nanocrystals from spruce bark in a biorefinery perspective, Carbohydrate polymers 111 (2014) 979-987.

[18] H. Kargarzadeh, I. Ahmad, I. Abdullah, A. Dufresne, S.Y. Zainudin, R.M. Sheltami, Effects of hydrolysis conditions on the morphology, crystallinity, and thermal stability of cellulose nanocrystals extracted from kenaf bast fibers, Cellulose 19(3) (2012) 855-866.

[19] H.-Y. Yu, Z.-Y. Qin, Y.-N. Liu, L. Chen, N. Liu, Z. Zhou, Simultaneous improvement of mechanical properties and thermal stability of bacterial polyester by cellulose nanocrystals, Carbohydrate polymers 89(3) (2012) 971-978.

[20] A. Arias, M.-C. Heuzey, M.A. Huneault, G. Ausias, A. Bendahou, Enhanced dispersion of cellulose nanocrystals in melt-processed polylactide-based nanocomposites, Cellulose 22(1) (2015) 483-498.

[21] M. Pracella, M.M.-U. Haque, D. Puglia, Morphology and properties tuning of PLA/cellulose nanocrystals bio-nanocomposites by means of reactive functionalization and blending with PVAc, Polymer 55(16) (2014) 3720-3728.

[22] E. Espino-Pérez, J. Bras, V. Ducruet, A. Guinault, A. Dufresne, S. Domenek, Influence of chemical surface modification of cellulose nanowhiskers on thermal, mechanical, and barrier properties of poly (lactide) based bionanocomposites, European Polymer Journal 49(10) (2013) 3144-3154.

[23] H. Yu, C. Yan, J. Yao, Fully biodegradable food packaging materials based on functionalized cellulose nanocrystals/poly (3-hydroxybutyrate-co-3-hydroxyvalerate) nanocomposites, RSC Advances 4(104) (2014) 59792-59802.

[24] D. Wang, J. Yu, J. Zhang, J. He, J. Zhang, Transparent bionanocomposites with improved properties from poly (propylene carbonate)(PPC) and cellulose nanowhiskers (CNWs), Composites Science and Technology 85 (2013) 83-89.

[25] G. Siqueira, J. Bras, A. Dufresne, Cellulose whiskers versus microfibrils: influence of the nature of the nanoparticle and its surface functionalization on the thermal and mechanical properties of nanocomposites, Biomacromolecules 10(2) (2008) 425-432.

[26] D. Garcia-Garcia, J. Ferri, T. Boronat, J. López-Martínez, R. Balart, Processing and characterization of binary poly (hydroxybutyrate)(PHB) and poly (caprolactone)(PCL) blends with improved impact properties, Polymer Bulletin 73(12) (2016) 3333-3350.

[27] A.M. Donald, E.J. Kramer, Plastic deformation mechanisms in poly (acrylonitrile-butadiene styrene)[ABS], Journal of Materials Science 17(6) (1982) 1765-1772.

[28] D. Garcia-Garcia, E. Rayón, A. Carbonell-Verdu, J. Lopez-Martinez, R. Balart, Improvement of the compatibility between poly (3-hydroxybutyrate) and poly (ε-caprolactone) by reactive extrusion with dicumyl peroxide, European Polymer Journal 86 (2017) 41-57.

[29] D. dos Santos Rosa, M.R. Calil, C.d.G.F. Guedes, T.C. Rodrigues, Biodegradability of thermally aged PHB, PHB-V, and PCL in soil compostage, J Polym Environ 12(4) (2004) 239-245.

[30] F. Fenouillot, P. Cassagnau, J.-C. Majesté, Uneven distribution of nanoparticles in immiscible fluids: morphology development in polymer blends, Polymer 50(6) (2009) 1333-1350.

[31] M. Arrieta, E. Fortunati, F. Dominici, E. Rayón, J. López, J. Kenny, Multifunctional PLA–PHB/cellulose nanocrystal films: processing, structural and thermal properties, Carbohydrate polymers 107 (2014) 16-24.

[32] M. Arrieta, E. Fortunati, F. Dominici, E. Rayón, J. López, J. Kenny, PLA-PHB/cellulose based films: Mechanical, barrier and disintegration properties, Polymer Degradation and Stability 107 (2014) 139-149.

[33] D. Li, R. Moriana, M. Ek, From forest residues to hydrophobic nanocomposites with high oxygen-barrier properties, Nord Pulp Pap Res J 31(2) (2016) 261-269.

[34] M. Arrieta, M. Samper, J. López, A. Jiménez, Combined Effect of Poly(hydroxybutyrate) and Plasticizers on Polylactic acid Properties for Film Intended for Food Packaging, J Polym Environ 22(4) (2014) 460-470.

[35] C.L. Simoes, J.C. Viana, A.M. Cunha, Mechanical Properties of Poly(epsilon-caprolactone) and Poly(lactic acid) Blends, Journal of Applied Polymer Science 112(1) (2009) 345-352.

[36] I.T. Seoane, E. Fortunati, D. Puglia, V.P. Cyras, L.B. Manfredi, Development and characterization of bionanocomposites based on poly (3-hydroxybutyrate) and cellulose nanocrystals for packaging applications, Polymer International 65(9) (2016) 1046-1053.

[37] Y. Chen, C. Liu, P.R. Chang, X. Cao, D.P. Anderson, Bionanocomposites based on pea starch and cellulose nanowhiskers hydrolyzed from pea hull fibre: effect of hydrolysis time, Carbohydrate Polymers 76(4) (2009) 607-615.

[38] M. Atef, M. Rezaei, R. Behrooz, Preparation and characterization agar-based nanocomposite film reinforced by nanocrystalline cellulose, International journal of biological macromolecules 70 (2014) 537-544.

[39] W. Yang, F. Dominici, E. Fortunati, J. Kenny, D. Puglia, Effect of lignin nanoparticles and masterbatch procedures on the final properties of glycidyl methacrylate-g-poly (lactic acid) films before and after accelerated UV weathering, Industrial Crops and Products 77 (2015) 833-844.

[40] M. Arrieta, E. Fortunati, F. Dominici, J. López, J. Kenny, Bionanocomposite films based on plasticized PLA–PHB/cellulose nanocrystal blends, Carbohydrate polymers 121 (2015) 265-275.

[41] E.A. Vogler, Structure and reactivity of water at biomaterial surfaces, Advances in colloid and interface science 74(1) (1998) 69-117.

[42] A. de Campos, G.H. Tonoli, J.M. Marconcini, L.H. Mattoso, A. Klamczynski, K.S. Gregorski, D. Wood, T. Williams, B.-S. Chiou, S.H. Imam, TPS/PCL composite reinforced with treated sisal fibers: property, biodegradation and water-absorption, J Polym Environ 21(1) (2013) 1-7.

[43] Y. Mo, R. Guo, J. Liu, Y. Lan, Y. Zhang, W. Xue, Y. Zhang, Preparation and properties of PLGA nanofiber membranes reinforced with cellulose nanocrystals, Colloids and Surfaces B: Biointerfaces 132 (2015) 177-184.

[44] D. García-García, A. Carbonell, M. Samper, D. García-Sanoguera, R. Balart, Green composites based on polypropylene matrix and hydrophobized spend coffee ground (SCG) powder, Composites Part B: Engineering 78 (2015) 256-265.

[45] M. Martínez-Sanz, M. Villano, C. Oliveira, M.G. Albuquerque, M. Majone, M. Reis, A. Lopez-Rubio, J.M. Lagaron, Characterization of polyhydroxyalkanoates synthesized from microbial mixed cultures and of their nanobiocomposites with bacterial cellulose nanowhiskers, New biotechnology 31(4) (2014) 364-376.

644 [46] H.-Y. Yu, J.-M. Yao, Reinforcing properties of bacterial polyester with different cellulose
645 nanocrystals via modulating hydrogen bonds, Composites Science and Technology 136 (2016)
646 53-60.

647 [47] H.-Y. Yu, H. Zhang, M.-L. Song, Y. Zhou, J. Yao, Q.-Q. Ni, From Cellulose Nanospheres,
648 Nanorods to Nanofibers: Various Aspect Ratio Induced Nucleation/Reinforcing Effects on
649 Polylactic Acid for Robust-Barrier Food Packaging, ACS applied materials & interfaces 9(50)
650 (2017) 43920-43938.

651 [48] H.-Y. Yu, C. Wang, S.Y.H. Abdalkarim, Cellulose nanocrystals/polyethylene glycol as
652 bifunctional reinforcing/compatibilizing agents in poly (lactic acid) nanofibers for controlling
653 long-term in vitro drug release, Cellulose 24(10) (2017) 4461-4477.

654 [49] L. Wei, N.M. Stark, A.G. McDonald, Interfacial improvements in biocomposites based on
655 poly (3-hydroxybutyrate) and poly (3-hydroxybutyrate-co-3-hydroxyvalerate) bioplastics
656 reinforced and grafted with α-cellulose fibers, Green chemistry 17(10) (2015) 4800-4814.

657 [50] H.S. Barud, J.L. Souza, D.B. Santos, M.S. Crespi, C.A. Ribeiro, Y. Messaddeq, S.J. Ribeiro,
658 Bacterial cellulose/poly (3-hydroxybutyrate) composite membranes, Carbohydrate Polymers
659 83(3) (2011) 1279-1284.

660 [51] A. Cano, E. Fortunati, M. Cháfer, C. González-Martínez, A. Chiralt, J. Kenny, Effect of cellulose
661 nanocrystals on the properties of pea starch–poly (vinyl alcohol) blend films, Journal of materials
662 science 50(21) (2015) 6979-6992.

663 [52] J. Xu, B.-H. Guo, R. Yang, Q. Wu, G.-Q. Chen, Z.-M. Zhang, In situ FTIR study on melting and
664 crystallization of polyhydroxyalkanoates, Polymer 43(25) (2002) 6893-6899.

665 [53] L. Wei, A.G. McDonald, N.M. Stark, Grafting of bacterial polyhydroxybutyrate (PHB) onto
666 cellulose via in situ reactive extrusion with dicumyl peroxide, Biomacromolecules 16(3) (2015)
667 1040-1049.

668 [54] B. Vergara-Porras, J.N. Gracida-Rodríguez, F. Pérez-Guevara, Thermal processing influence
669 on mechanical, thermal, and biodegradation behavior in poly (β-hydroxybutyrate)/poly (ε-
670 caprolactone) blends: A descriptive model, Journal of Applied Polymer Science 133(27) (2016).

671 [55] C. Del Gaudio, E. Ercolani, F. Nanni, A. Bianco, Assessment of poly (ε-caprolactone)/poly (3-
672 hydroxybutyrate-co-3-hydroxyvalerate) blends processed by solvent casting and
673 electrospinning, Materials Science and Engineering: A 528(3) (2011) 1764-1772.

674 [56] M.P. Cavalcante, A.L. Toledo, E.J. Rodrigues, R.P. Neto, M.I. Tavares, Correlation between
675 traditional techniques and TD-NMR to determine the morphology of PHB/PCL blends, Polymer
676 Testing 58 (2017) 159-165.

677 [57] Y. Dasan, A. Bhat, F. Ahmad, Polymer blend of PLA/PHBV based bionanocomposites
678 reinforced with nanocrystalline cellulose for potential application as packaging material,
679 Carbohydrate polymers 157 (2017) 1323-1332.

680 [58] D. Puglia, E. Fortunati, D.A. D'amico, L.B. Manfredi, V.P. Cyras, J. Kenny, Influence of
681 organically modified clays on the properties and disintegrability in compost of solution cast poly
682 (3-hydroxybutyrate) films, Polymer Degradation and Stability 99 (2014) 127-135.
683